Soft Matter

PAPER

View Article Online
View Journal | View Issue

Cite this: *Soft Matter*, 2014, **10**, 5715

Rationally designed anion-responsive-organogels: sensing F^- *via* reversible color changes in gel–gel states with specific selectivity†

Qi Lin,*[a] Xin Zhu,[a] Yong-Peng Fu,[a] You-Ming Zhang,[a] Ran Fang,[b] Li-Zi Yang[b] and Tai-Bao Wei*[a]

Received 17th April 2014
Accepted 28th May 2014

DOI: 10.1039/c4sm00841c

www.rsc.org/softmatter

Through the rational introduction of the multi self-assembly driving forces and F^- sensing sites into a gelator molecule, low-molecular-weight organogelators **L1** and **L2** were designed and synthesized. **L1** and **L2** showed excellent gelation ability in DMF and DMSO. They could form stable organogels (**OGL1** and **OGL2**) in DMF and DMSO with very low critical gelation concentrations. **OGL1** and **OGL2** could act as anion-responsive organogels (AROGs). Unlike most of the reported AROGs showing gel–sol phase transition according to the anions' stimulation, **OGL1** could colorimetrically sense F^- under gel–gel states. Upon addition of F^-, **OGL1** showed dramatic color changes, while the color could be recovered by adding H^+. Moreover, **OGL1** showed specific selectivity for F^-, other common anions and cations could not lead to any similar response. What deserves to be mentioned is that the report on specific sensing of anions under gel–gel states is very scarce. The gel–gel state recognition can endow the organogel **OGL1** with the merits of facile and efficient properties for rapid detection of F^-. Therefore, **OGL1** could act as a F^- responsive smart material.

1. Introduction

Smart materials which can sense, process, and actuate a response to an external change without assistance have been attracting considerable attention due to their wide range of potential applications in sensors, biomaterials, surface science, displays, *etc.*[1–3] Among them, stimuli-responsive supramolecular organogels are one kind of the most attractive examples.[4–10] Supramolecular organogels are formed by assembling low-molecular-weight gelators (LMWGs) into physically crosslinked three-dimensional networks with solvent molecules entrapped inside through noncovalent intermolecular interactions, such as hydrogen bonding, π–π stacking, van der Waals (vdW), electrostatic interactions, and so on.[11–19] Due to the weak nature of these forces, the gel–sol transition of organogels is thermally reversible and can be further tuned by other physical and chemical stimuli. These intriguing properties of organogels endow them with promising applications in optoelectronic devices, template syntheses, drug delivery, tissue engineering, catalysis, and biomimetic systems.[20–24] Despite the great progress made recently in this field, there are two big challenges in the field of designing novel organogels. One is how to improve the gelator's gelation ability and make sure that the designed gelator can self-assemble into the desired organogel in certain solutions and the other is how to selectively detect a given chemical stimulus.

In addition, anions play a fundamental role in chemical, biological and environmental processes. More and more interest has been attracted in selective recognition and sensing of anions *via* artificial receptors.[25–35] Among the anions, fluoride anions are one of the most attractive targets because of their considerable significance for health and environmental issues.[36] Therefore, there is a great demand for the development of methods that can rapidly, sensitively, and selectively detect the fluoride anion.[37,38] As we all know, an important feature of the chemosensor is its specific selectivity toward the analyte. Although considerable efforts have been made for the development of anion-responsive organogel (AROG),[4–10,12,15,39–44] few AROGs could detect fluoride anions with specific selectivity.

Moreover, common AROGs realize the anion recognition *via* a reversible or irreversible gel–sol phase transition because the anion could be competitively bound to the gelator's self-assembly sites (*e.g.*, hydrogen bonds or electrostatic interactions sites) and induce the dis-assembly of the organogel. To date, the reports of supramolecular organogel which could colorimetrically or fluorescently detect anions under gel–gel states without sol–gel phase change are very scarce. What is

[a]*Key Laboratory of Eco-Environment-Related Polymer Materials, Ministry of Education of China, Key Laboratory of Polymer Materials of Gansu Province, College of Chemistry and Chemical Engineering, Northwest Normal University, Lanzhou, Gansu, 730070, P. R. China. E-mail: linqi2004@126.com; weitaibao@126.com*

[b]*College of Chemistry and Chemical Engineering, Lanzhou University, Lanzhou, Gansu, 730070, P. R. China*

† Electronic supplementary information (ESI) available. See DOI: 10.1039/c4sm00841c

more the gel–gel state recognition can endow the AROGs with the merits of facile and efficient properties for rapid detection of the target anion.

In view of this, as a part of our research interest in molecular recognition,[43,45–49] herein, we report an AROG which could selectively recognize F^- *via* a dramatic color change under gel–gel states, the color could be recovered by adding H^+. It is interesting to note that in the F^- recognition process, the organogel did not carry out gel–sol phase change. In addition, other anions (such as AcO^-, $H_2PO_4^-$, Cl^-, Br^-, I^-, HSO_4^- and ClO_4^-) and common cations (such as Mg^{2+}, Ca^{2+}, Cr^{3+}, Fe^{3+}, Co^{2+}, Ni^{2+}, Cu^{2+}, Zn^{2+}, Ag^+, Cd^{2+}, Hg^{2+} and Pb^{2+}) could not lead to any similar response. Our strategy for the design of gelator **L1** (Scheme 1) is as follows. Firstly, in order to achieve specific selectivity for F^-, we rationally selected and introduced an F^- sensing group into the gelator molecule. There are lots of functional groups have been reported as F^- sensing groups, like urea, thiourea, amide, phenol, pyrrole, acylhydrazone and arylhydrazone and so on.[37,38] Among them, the hydrazone group (–CH=N–NH–), as a sense site, possesses several merits. For example, there are two different hydrogen bond donor sites (H–C=N– and –N–H) in the same group, both of which can act as anion binding sites as well as self-assembly sites. Furthermore, owing to the fact that the acidity of "–N–H" is stronger than that of "H–C=N–", the hydrazone group can sense F^- not only by forming hydrogen bonds ($F^-\cdots$H–C=N–) but also by a deprotonation process (deprotonation of –N–H). As a result, it can afford two kinds of sense approaches and enhance the sense selectivity for F^-. In the light of these considerations, we introduced hydrazone groups into the gelator as F^- sensing sites and hydrogen bond donor groups. Secondly, in order to obtain easy gelation and a relatively stable gelator, we introduced a 3,4-bis(hexadecyloxy)phenyl group as a self-assembly group to provide strong vdW forces. In addition, since the arylhydrazone group and the 3,4-bis(hexadecyloxy)phenyl group were introduced into the same gelator molecule, the gelator possesses three kinds of self-assembly driving forces, including vdW forces, hydrogen bonding and π–π stacking interactions. These designs provided the gelator **L1** with stronger gelation ability. Finally, with the aim to achieve colorimetric sense for F^-, a nitrophenyl group was introduced into the gelator as a colorimetric signal group.

2. Experimental section

Synthesis of L1

3,4-Bis(hexadecyloxy)benzaldehyde was synthesized according to literature methods.[50,51] 3,4-Bis(hexadecyloxy)benzaldehyde (5.0 mmol), 4-nitrobenzenehydrazine (5.0 mmol) and a catalytic amount of *p*-toluenesulfonic acid (*p*-Ts) were mixed in hot absolute ethanol (30 mL). The solution was stirred under reflux conditions for 8 hours. After being cooled to room temperature, the yellow precipitate was filtered and then recrystallized with $CHCl_3$–EtOH to get compound **L1** (yield, 72%) as an orange powdery product: ^{1}H NMR ($CDCl_3$, 400 MHz) δ 8.18 (d, J = 6.9 Hz, 2H, ArH), 7.91 (s, 1H, –NH), 7.70 (s, 1H, –N=CH–), 7.33 (s, 1H, ArH), 7.10–7.07 (m, 3H, ArH), 6.87 (d, J = 6.3 Hz, 1H, ArH), 4.06 (m, 4H, $-OCH_2$), 1.86 (m, 4H, $-OCH_2CH_2$), 1.51 (m, 4H, $-CH_2CH_3$),1.35 (m, 48H, $-C_{12}H_{24}$), 0.87 (t, J = 5.4 Hz, 6H, $-CH_2CH_3$); ^{13}C NMR ($CDCl_3$, 150 MHz) δ 150.85, 149.56, 149.37, 141.75, 139.93, 126.86, 126.25, 121.29, 112.75, 111.43, 110.26, 69.23, 31.88, 29.36, 25.99, 22.65, 14.10; IR (KBr, cm^{-1}) ν: 3505 (N–H), 2919, 2850 (C–H), 1596 (C=N), 1516, 1468 (C=C), 1111 (Ar–O–C). Anal. calcd for $C_{45}H_{75}N_3O_4$: C 74.85, H 10.47, N 5.82; found C, 74.88, H, 10.41, N, 5.85. MS: m/z: 722.9 [**L1** + H]$^+$; calcd for $C_{45}H_{76}N_3O_4$: 722.6.

Synthesis of L2

The compound **L2** (yield, 85%) was prepared by a similar procedure: ^{1}H NMR ($CDCl_3$, 400 MHz) δ 11.30 (s, 1H, –NH), 9.16 (s, 1H, –N=CH–), 8.35 (d, J = 7.2 Hz, 1H, ArH), 8.06 (d, J = 11.6 Hz, 2H, ArH), 7.38 (s, 1H, ArH), 7.19 (d, J = 8.4 Hz, 1H, ArH), 6.91 (d, J = 8.4 Hz, 1H, ArH), 4.10–4.04 (m, 4H, $-OCH_2$), 1.89–1.84 (m, 4H, $-OCH_2CH_2$), 1.53–1.49 (m, 4H, $-CH_2CH_3$), 1.37–1.25 (m, 48H, $-C_{12}H_{24}$), 0.89 (t, J = 6.4 Hz, 6H, $-CH_2CH_3$). ^{13}C NMR ($CDCl_3$, 150 MHz) δ 152.09, 149.46, 148.35, 144.72, 137.79, 137.23, 129.93, 128.97, 125.67, 122.76, 116.56, 112.60, 110.82, 69.32, 31.91, 29.66, 29.36, 25.99, 22.68, 14.11; IR (KBr, cm^{-1}) ν: 3443 (N–H), 2920, 2849 (C–H), 1616 (C=N), 1508, 1466 (C=C), 1133 (Ar–O–C). Anal. calcd for $C_{45}H_{74}N_4O_6$: C 70.46, H 9.72, N 7.30; found C, 70.48, H, 9.70, N, 7.25. MS: m/z: 767.9 [**L2** + H]$^+$; calcd for $C_{45}H_{75}N_4O_6$: 767.6.

3. Results and discussion

The gelation abilities of gelators **L1** and **L2** were examined in various solvents by means of the "stable to inversion of a test

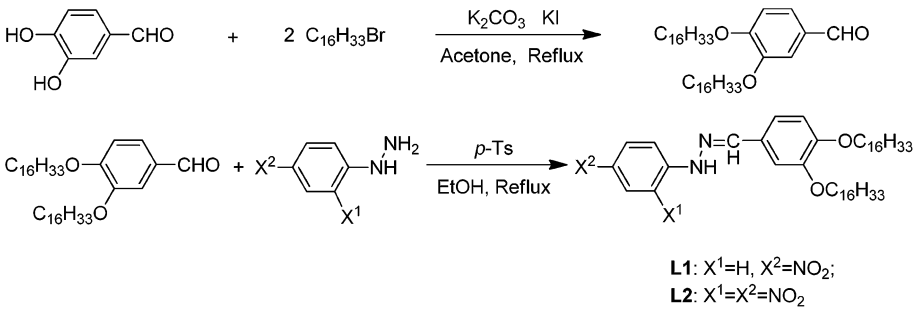

Scheme 1 Structure and synthesis of the gelators L1 and L2.

Table 1 Gelation properties of L1 and L2

	L1	L2
Solvent	State[a] (CGC[b], CGT[c])	State (CGC, CGT)
n-Amyl alcohol	I	I
Ethanol	P	I
Acetone	S	I
Acetonitrile	P	I
DMSO	OG (0.6%, 58 °C)	OG (0.2%, 75 °C)
Toluene	S	S
Petroleum ether	P	P
THF	S	S
Chloroform	S	P
Dichloromethane	WG	P
Cyclohexanol	I	I
DMF	OG (3.1%, 38 °C)	OG (1.7%, 65 °C)

[a] OG, opaque gel; S, solution; I, insoluble; WG, weak gel; P, precipitate.
[b] CGC is the critical gelation concentration (w/v%, 10 mg mL^{-1} = 1%).
[c] CGT is the gelation temperature (°C) at critical gelation concentration.

tube" method. The corresponding critical gelation concentrations (CGCs) at room temperature were also measured (Table 1). Gelators **L1** and **L2** could gel polar aprotic solvents dimethyl sulfoxide (DMSO) and *N*,*N*-dimethylformamide (DMF). More interestingly, **L1** and **L2** exhibited excellent gelation abilities and very low CGCs in DMSO, and the CGCs of **L1** and **L2** were 0.6% and 0.2% respectively. Moreover, in DMSO, the sol–gel transition was very rapid. The whole transition process only took less than 3 min after heating of the DMSO solution was stopped. The gel–sol transition temperature (T_{gel}) was measured by using the 'tilted tube' method. Regularly increasing the concentration of **L1** and **L2** led the T_{gel} to reach a limit of 79 °C and 111 °C respectively (Fig. 1). These gels were found stable in closed tubes for at least 3 months at 25 °C. According to the CGCs and T_{gel} of **L1** and **L2**, we could find that **L2** was more stable than **L1**, because **L2** contained more nitro groups than **L1** and the nitro groups could act as the hydrogen bond acceptor for these gelators.

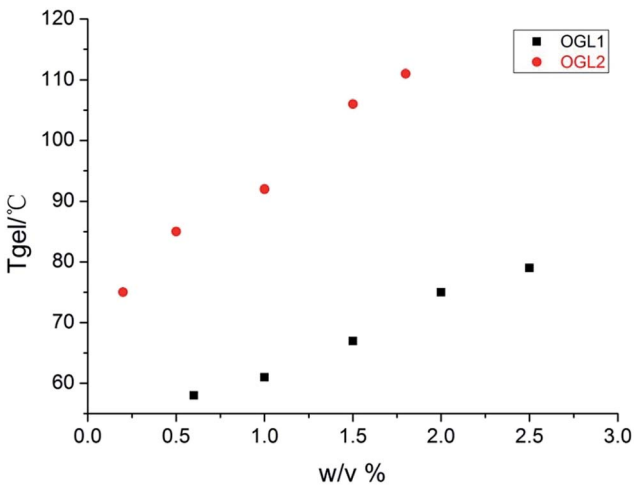

Fig. 1 Plots of T_{gel} *versus* the concentration of OGL1 and OGL2 obtained from DMSO.

Since gelators **L1** and **L2** could form stable organogel in DMSO, a series of experiments were carried out to investigate the anion response capability of the organogels formed by gelators **L1** and **L2** in DMSO (named **OGL1** and **OGL2** respectively). As we expected, **OGL1** and **OGL2** exhibited excellent color changes according to the stimulus of the fluoride ion. As shown in Fig. 2, upon addition of F^- (5 equiv., solid Bu_4NF) to **OGL1** at 25 °C, a dramatic color change from yellow to dark brown instantly took place on the surface of **OGL1**. The color of whole gels changed in *ca.* 4 hours with F^- diffusion into the gels. Additionally, the color of **OGL1** could be recovered by adding proton solutions such as $HClO_4$ solution, MeOH or water. It is very interesting that unlike most of the reported AROGs which showed gel to solution phase transition according to the fluoride anion's stimulation, the gel state of **OGL1** did not show any changes in the whole F^- response process. The T_{gel} of F^--contained gel is 52 °C and the hot solution of F^--contained gel could recover to the gel states after cooling the sol to room temperature. This special stability could be attributed to the cooperation of the above-mentioned multi self-assembly forces (vdW forces, hydrogen bonding and π–π stacking interactions) we rationally introduced into the gelators. Simply stated, because there are three kinds of self-assembly driving forces in the same gelator, even if the hydrogen bonds were destroyed by F^-, the remaining two forces could maintain the organogels' gel states. Meanwhile, owing to the breaking of hydrogen bonds, the T_{gel} of **OGL1** changed from 79 °C to 52 °C. Under the same conditions, **OGL2** showed similar response for F^-.

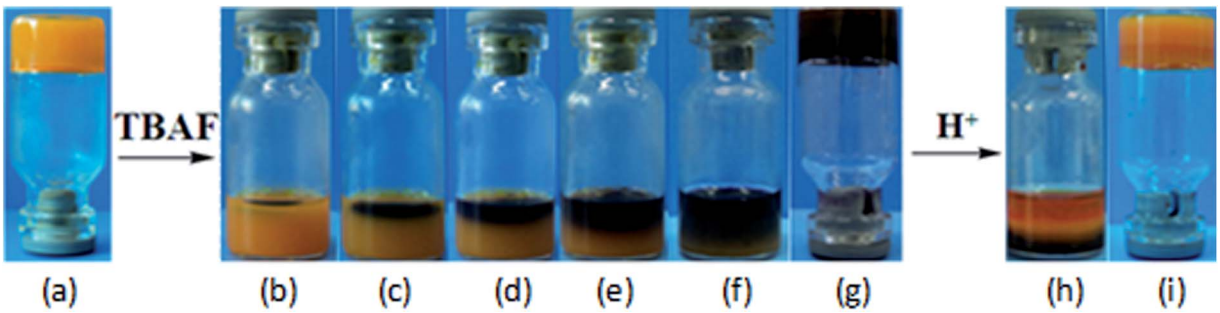

Fig. 2 (a) Organogel **OGL1** (0.8%, in DMSO); (b) immediately after addition of solid TBAF (5 equiv.); (c) after 30 min; (d) after 90 min; (e) after 150 min; (f and g) after 220 min; (h) addition of 0.05 mL $HClO_4$ (0.01 M) after 10 min; (i) after 20 min.

The selectivity of organogels for anions was also investigated. As shown in Fig. 3, when DMSO solutions of various anions (F^-, Cl^-, Br^-, I^-, AcO^-, $H_2PO_4^-$, HSO_4^- and ClO_4^-) were added to the small amounts of organogel **OGL1** on a spot plate, only F^- could induce an instant color change of **OGL1**. Other anions could not induce any color or organogels' state change, which indicated that **OGL1** could instantly sense F^- with specific selectivity. The selectivity tests were also carried out in the DMSO solution of gelator **L1**. As shown in Fig. 4, in DMSO solution, the gelator **L1** could selectively respond to F^- by color change. In the corresponding UV-vis spectra, upon addition of F^-, the absorption of **L1** at 430 nm shifted to 570 nm. Similarly, the color and the UV-vis absorption could be restored by adding proton solutions (Fig. S1a in the ESI†). As shown in Fig. 4 and 5, other anions (Cl^-, Br^-, I^-, AcO^-, $H_2PO_4^-$, HSO_4^- and ClO_4^-) and common cations (such as Mg^{2+}, Ca^{2+}, Cr^{3+}, Fe^{3+}, Co^{2+}, Ni^{2+}, Cu^{2+}, Zn^{2+}, Ag^+, Cd^{2+}, Hg^{2+} and Pb^{2+}) could not cause any significant color or spectral response. Therefore, the gelator **L1** could respond to F^- with specific selectivity. However, under similar conditions, the addition of AcO^- or $H_2PO_4^-$ also led to the color of **OGL2** changing from yellow to red (Fig. 4) and the color and UV-vis absorption could be restored by adding proton solutions too (Fig. S1b in the ESI†). Thus, **OGL2** could respond to F^-, AcO^- and $H_2PO_4^-$ without specific selectivity.

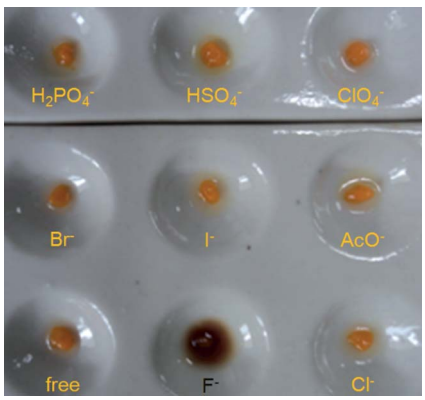

Fig. 3 Color changes immediately after the addition of various anions (one drop, *ca.* 0.02 mL) to organogel **OGL1** (0.8%, in DMSO) on a spot plate.

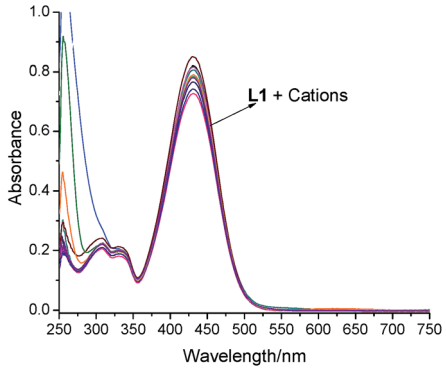

Fig. 5 UV-vis spectra of **L1** (2.0×10^{-55} M) in DMSO upon addition of 10 equiv. of various cations (Mg^{2+}, Ca^{2+}, Cr^{3+}, Fe^{3+}, Co^{2+}, Ni^{2+}, Cu^{2+}, Zn^{2+}, Ag^+, Cd^{2+}, Hg^{2+} and Pb^{2+}).

According to these results we can find that **L1** and **L2** showed different anion response selectivities. Because in the molecule of **L2**, there is an intramolecular hydrogen bond between hydrazone –N–H and *ortho* nitro groups (Fig. 6). This hydrogen bond enhanced the acidity of the –N–H group. Therefore, the –N–H group in **L2** could carry out a deprotonation process not only with F^- but also with AcO^- and $H_2PO_4^-$. This assumption was confirmed by ^{1}H NMR spectra. The –N–H proton chemical shift of **L1** appeared at 7.91 ppm, while in **L2** the –N–H signal appeared at 11.30 ppm, which indicated that the –N–H group of **L2** more easily deprotonates than that of **L1**.

The anion response mechanisms of **L1** and **L2** were carefully investigated by various methods. According to the absorption titration experiments (Fig. 7a), upon gradual addition of F^- to the solution of **L1**, an isosbestic point at 475 nm was observed. Moreover, in Job's plots (Fig. 7b), the absorbance value approached the maximum when the molar fraction of **L1** was 0.5, which demonstrated the formation of a 1 : 1 complex between **L1** and F^-. By the Benesi–Hildebrand equation fitting[52]

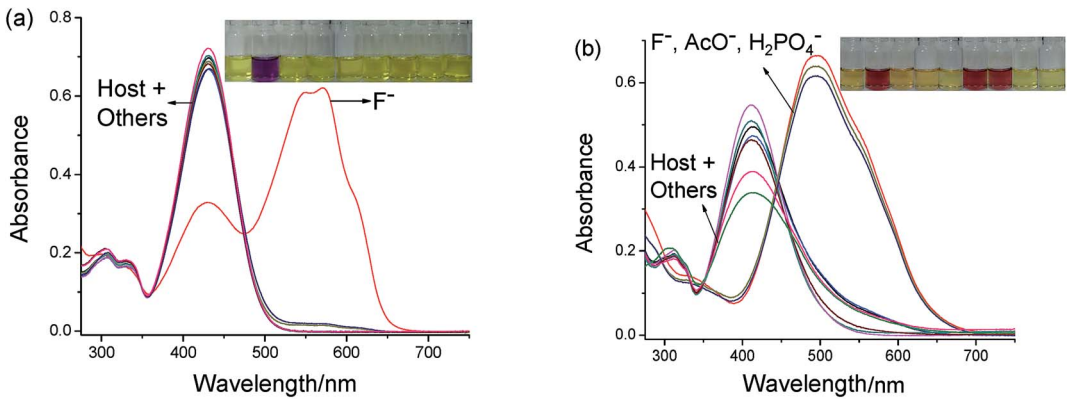

Fig. 4 UV-vis spectral response of (a) **L1**; (b) **L2** (2.0×10^{-5} M) in DMSO upon addition of 50 equiv. of various anions. Inset: photograph of (a) **L1**; (b) **L2** (2.0×10^{-5} M) upon adding 50 equiv. of various anions in DMSO, from left to right: none, F^-, Cl^-, Br^-, I^-, AcO^-, $H_2PO_4^-$, HSO_4^-, and ClO_4^-.

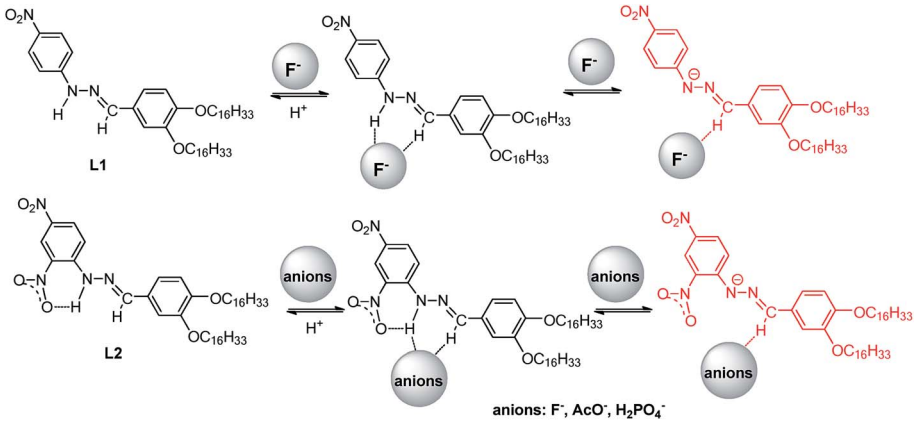

Fig. 6 A possible mechanism of **L1** and **L2** response to F^- or anions.

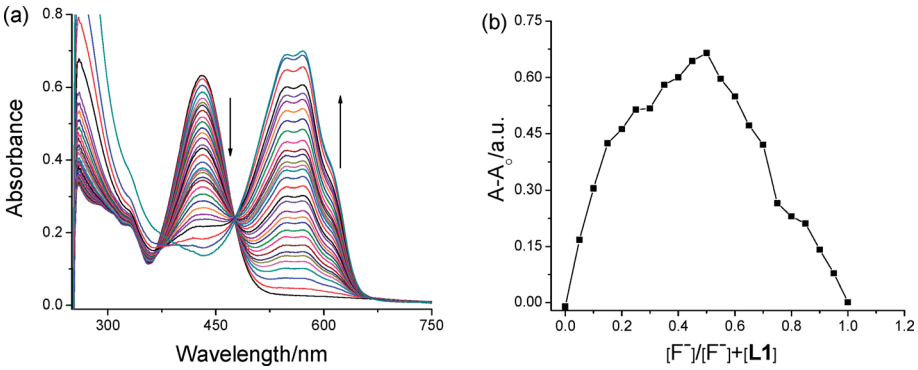

Fig. 7 (a) UV-vis spectral titration of **L1** (2.0×10^{-5} M) with F^- in DMSO solution. (b) Job's plot for the complex of **L1** and F^- (in DMSO solution), which indicated that the stoichiometry of **L1**–F^- is 1 : 1.

at $\lambda_{max} = 571$ nm for **L1**, the association constant K_a of **L1** with F^- was obtained as 1.67×10^3 M^{-1}.

The further **L1**–F^- reaction mechanism was investigated by F^-–^{1}H NMR titration, ^{19}F NMR and ESI-MS experiments. As shown in Fig. 8, in the F^-–^{1}H NMR titration spectra, before the addition of F^-, chemical shifts of the N–H and –HC=N– protons on **L1** appeared at δ 7.91 and 7.70 ppm. After the addition of 0.2 equiv. of F^-, the signal of these two protons shifted downfield.

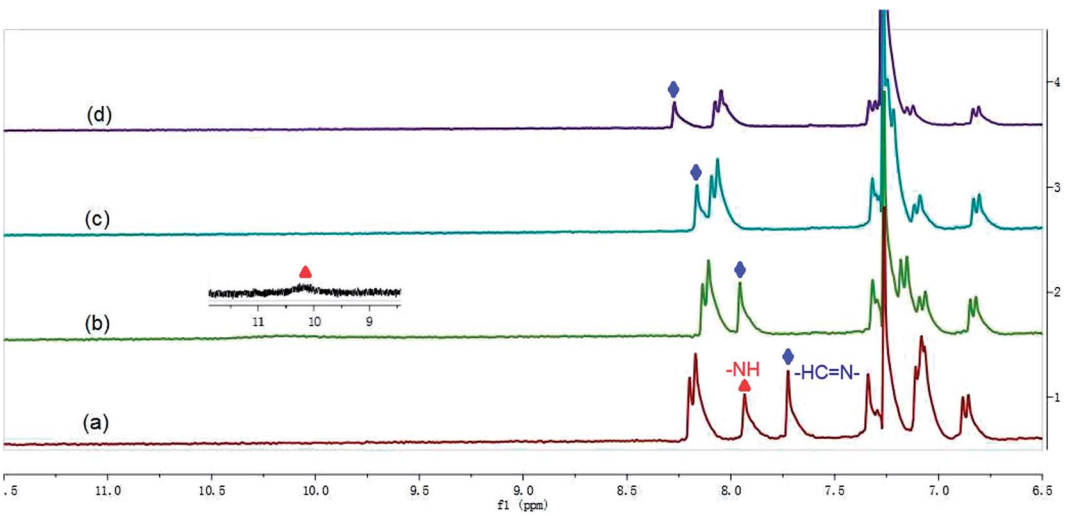

Fig. 8 Partial ^{1}H NMR spectra of **L1** (0.01 M) in $CDCl_3$ upon addition of F^-. (a) Free; (b) 0.2 equiv. of F^-; (c) 0.5 equiv. of F^-; (d) 1.0 equiv. of F^-.

With the continuous addition of F^-, the N–H signal completely disappeared; meanwhile, the –HC═N– signal shifted downfield at δ 8.30 ppm. These phenomena indicated that the N–H group might undergo a deprotonation process and the –HC═N– group formed a $F^-\cdots$H–C═N– hydrogen bond (Fig. 6). The deprotonation process induced the color changes of the **L1** solution and **OGL1**. This process could be confirmed by adding proton solutions to **OGL1** containing F^-. After adding proton solutions, the color of the solution or gel turned yellow again.

The presumed F^- response mechanism was also supported by ^{19}F NMR and EI-Mass. As shown in Fig. 9, in the ^{19}F NMR spectra of TBAF, the signal of F^- appeared at −129.36 ppm. While after the addition of 50 equiv. TBAF into the $CDCl_3$ solution of **L1**, two ^{19}F signals appeared in the corresponding ^{19}F NMR spectra at −129.03 and −81.56 ppm respectively. The signal at −126.03 was attributed to the excess TBAF and the signal at −81.56 was attributed to the **L1**–F^- complex. Meanwhile, in the ESI-MS spectra of sensor **L1**, the $[\mathbf{L1} + H]^+$ peak appeared at 722.9 (m/z calcd = 722.6). However, when 50 equiv. of F^- was added to the solution of **L1**, a new peak appeared at 764.7, coinciding well with that for the species $[\mathbf{L1} + F^- + Na^+ + H]^+$ (m/z calcd = 764.6) and indicating the formation of the stabilized anionic species **L1**–F^-.

Moreover, in order to provide more adequate evidence for the possible anion response mechanism, the ^{1}H NMR titration experiments of **L1** and **L2** with AcO^- were carried out. As shown in Fig. S2,† chemical shifts of the N–H and –HC═N– protons on **L1** appeared at δ 7.91 and 7.70 ppm. After the addition of 0.5 equiv. of AcO^-, the signal of these two protons shifted downfield. After the addition of 2 equiv. of AcO^-, the signal of these two protons shifted to 10.66 and 8.03 ppm, respectively.

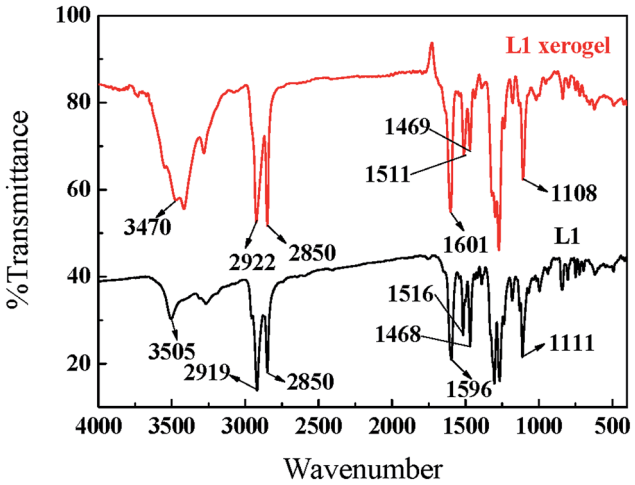

Fig. 11 FT-IR spectra of powdered **L1** and xerogel of **OGL1** (0.8% in DMSO).

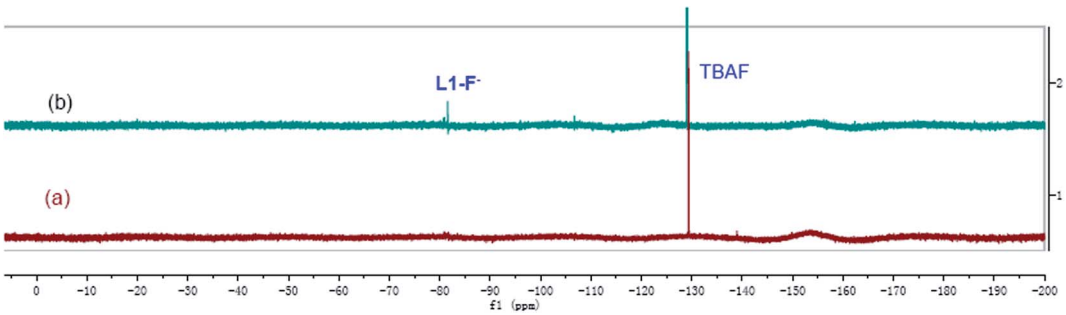

Fig. 9 Partial ^{19}F NMR spectra of (a) TBAF and (b) **L1** + TBAF (50 equiv.).

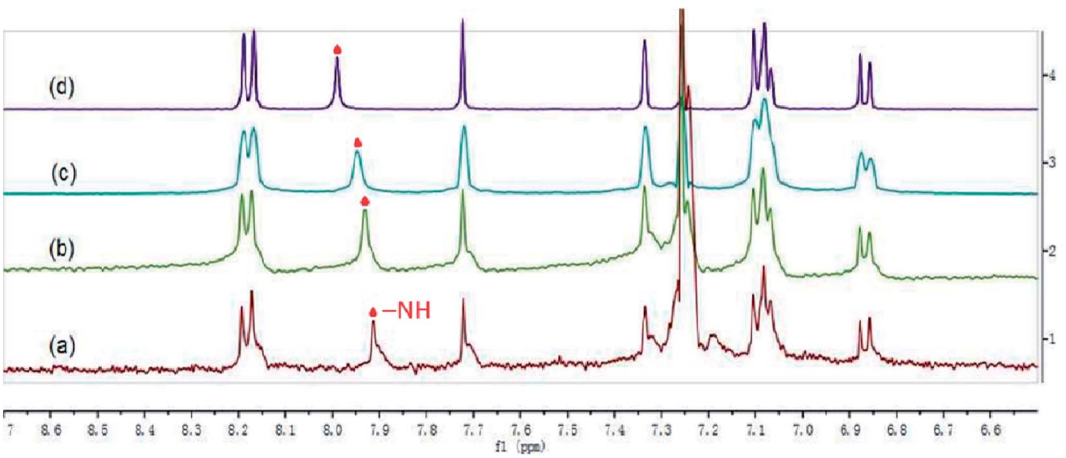

Fig. 10 Partial ^{1}H NMR spectra of **L1** in $CDCl_3$ with different concentrations (a) 0.6 mM; (b) 2.8 mM; (c) 13.9 mM; (d) 27.7 mM.

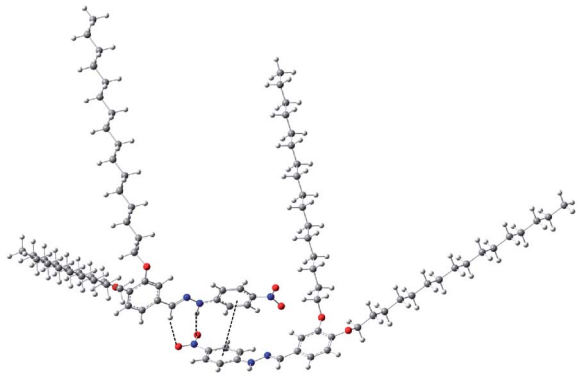

Fig. 12 Optimized self-assembly model of **OGL1** obtained by DFT calculations.

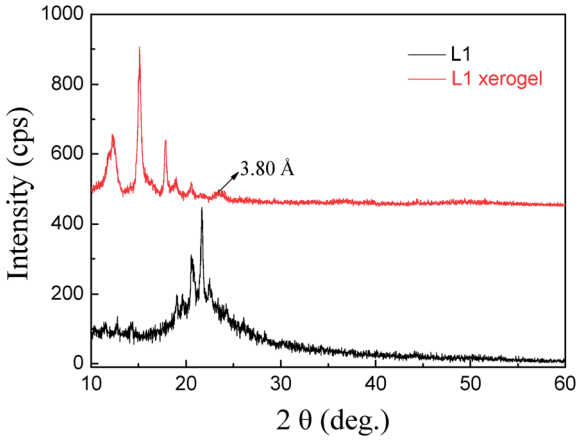

Fig. 13 Powder X-ray diffraction patterns for powdered **L1** and xerogel of **OGL1** (0.8% in DMSO).

These results indicated that the N–H and –HC═N– protons on **L1** formed stable hydrogen bonds with AcO^-. Thus, unlike that F^- could induce the deprotonation of N–H on **L1**, AcO^- could not deprotonate N–H of **L1**. Therefore, AcO^- could not lead to the color change of **L1** and **OGL1**. The similar experiments were carried out for **L2** with AcO^-. As shown in Fig. S3,† in the ^{1}H NMR spectra of **L2**, the N–H and –HC═N– protons on **L2** were at δ 11.3 and 9.16 ppm. Upon addition of AcO^-, the N–H signal at 11.3 ppm disappeared, indicating the deprotonation of the –N–H group. Usually, the deprotonation of the N–H group on the hydrazone moiety would induce the proton signal of –HC═N– shifted upfield while the formation of hydrogen bonds would induce the proton signal of –HC═N– shifted downfield. When the two events took place simultaneously, the signal of the –HC═N– group would not show an obvious shift. Upon addition of AcO^-, the –HC═N– proton signal of **L2** did not show obvious upfield-shift, which indicated that AcO^- formed hydrogen bonds with the –HC═N– group (Fig. 6).

The self-assembly mechanism was investigated by ^{1}H NMR, FT-IR, DFT calculations, X-ray diffraction and SEM. According to the results of concentration dependent ^{1}H NMR experiments (Fig. 10), the NH resonance signals gradually shifted downfield as the concentration of **L1** rose. Moreover, in the FT-IR spectra (Fig. 11) the N–H vibration absorption of powdery **L1** appeared at 3505 cm^{-1} while it shifted to 3470 cm^{-1} in xerogel. These results revealed that the NH groups formed hydrogen bonds in the gelation process.

These presumptions were confirmed by the optimized self-assembly model obtained by DFT calculations. As shown in Fig. 12, the nitro group on one gelator formed two intermolecular hydrogen bonds with the NH and CH groups on the other gelator molecule (bond length: –N–H···O, 14 Å; –C–H···O, 2.508 Å). There were π–π stacking interactions in neighbouring nitrophenyl groups, and the distance between the two phenyl groups was 3.84 Å. Therefore, the gelator **L1** could self-assemble into stable organogel *via* the hydrogen bonds, π–π stacking interactions, and vdW interactions.

Moreover, the X-ray diffraction patterns (Fig. 13) of **OGL1** xerogel showed periodical diffraction peaks, indicating that **L1** indeed assembled into an ordered structure. The *d*-spacing of 3.80 Å at $2\theta = 23.42$ suggested that π–π stacking existed between the phenyl groups of gelator **L1**, which also supported the self-assembly assumption.

The SEM images of **OGL1** showed a network structure consisting of many entangled tape-like structures. These tapes were approximately 10–30 nm in width and several μm long (Fig. 14a). It was very interesting that although the macro-phase of **OGL1** could not change under the stimulation of F^-, at the micro-level, the self-assembly process was actually influenced by F^-. As shown in (Fig. 14b), upon addition of F^-, the entangled tape-like structure (Fig. 14a) of **OGL1** changed to a rugate layer structure (Fig. 14b). This phenomenon could be attributed

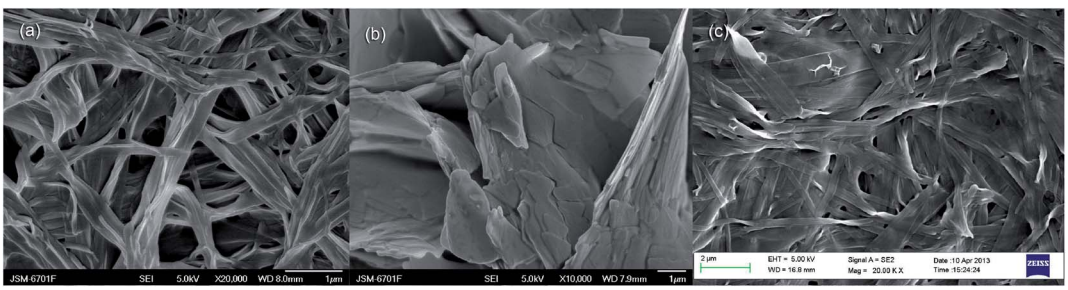

Fig. 14 SEM images of (a) xerogel of **OGL1** (0.8%, in DMSO); (b) **OGL1** xerogel treated with F^- *in situ*; (c) **OGL1** xerogel treated with F^- *in situ*, then added $HClO_4$ (0.01 M).

to the deprotonation of the N–H group by the attack of F^-. When the N–H group was deprotonated, the hydrogen bonds between the gelators were destroyed, and the gelators were assembled by vdW forces among long alkyl chains and π–π stacking interactions among nitrophenyl groups. Therefore, the micro-morphology of **OGL1** changed as mentioned above. When adding the proton solutions ($HClO_4$, H_2O, *etc.*) to **OGL1** containing F^-, the micro-morphology was restored (Fig. 14c).

4. Conclusion

In summary, we have developed an excellent organogel **OGL1** which could act as a F^- responsive smart material for instant colorimetric detection of F^- with specific selectivity under gel–gel states as well as in DMSO solutions. The color change induced by F^- could be recovered by adding proton solutions. Other anions and common cations did not cause any similar stimuli response. With the cooperation of multi self-assembly driving forces we rationally introduced into the gelator, **L1** showed excellent gelation capability in DMSO and DMF. Of particular significance, in the F^- sensing process, the organogel did not carry out any gel–sol phase change at the macro-level, which is very rare in the research of anion responsive organogels. The gel–gel state recognition has the merits of facile and efficient properties. The experimental study presented herein has important potential for the fabrication of smart materials in anion sensing applications.

Acknowledgements

We are grateful for financial support from the National Natural Science Foundation of China (NSFC) (nos 21064006; 21161018; 21262032), the Natural Science Foundation of Gansu Province (1308RJZA221) and the Program for Changjiang Scholars and Innovative Research Team in the University of Ministry of Education of China (IRT1177).

References

1 S. Landsmann, M. Wessig, M. Schmid, H. Cöfen and S. Polarz, *Angew. Chem., Int. Ed.*, 2012, **51**, 5995.
2 J. A. Hubbell and A. Chilkoti, *Science*, 2012, **337**, 303.
3 T. Aida, E. W. Meijer and S. I. Stupp, *Science*, 2012, **335**, 813.
4 G. O. Lloyd and J. W. Steed, *Nat. Chem.*, 2009, **1**, 437.
5 X. F. Ji, Y. Yao, J. Y. Li, X. Z. Yan and F. H. Huang, *J. Am. Chem. Soc.*, 2013, **135**, 74.
6 H. Maeda, *Chem.–Eur. J.*, 2008, **14**, 11274.
7 X. Z. Yan, F. Wang, B. Zheng and F. H. Huang, *Chem. Soc. Rev.*, 2012, **41**, 6042.
8 J. M. Hu, G. Q. Zhang and S. Y. Liu, *Chem. Soc. Rev.*, 2012, **41**, 5933.
9 Z. X. Liu, Y. Feng, Z. C. Yan, Y. M. He, C. Y. Liu and Q. H. Fan, *Chem. Mater.*, 2012, **24**, 3751.
10 M. D. Segarra-Maset, V. J. Nebot, J. F. Miravet and B. Escuder, *Chem. Soc. Rev.*, 2013, **42**, 7086.
11 F. H. Huang and O. A. Scherman, *Chem. Soc. Rev.*, 2012, **41**, 5879.
12 L. E. Buerklea and S. J. Rowan, *Chem. Soc. Rev.*, 2012, **41**, 6089.
13 G. C. Yu, X. Z. Yan, C. Y. Han and F. H. Huang, *Chem. Soc. Rev.*, 2013, **42**, 6697.
14 Y. L. Liu, Z. Q. Wang and X. Zhang, *Chem. Soc. Rev.*, 2012, **41**, 5922.
15 M.-O. M. Piepenbrock, G. O. Lloyd, N. Clarke and J. W. Steed, *Chem. Rev.*, 2010, **110**, 1960.
16 J. W. Steed, *Chem. Commun.*, 2011, **47**, 1379.
17 J. Liu, Yu. Feng, Z. X. Liu, Z. C. Yan, Y. M. He, C. Y. Liu and Q. H. Fan, *Chem.–Asian J.*, 2013, **8**, 572.
18 J. Zeng, W. Wang, P. Deng, W. Feng, J. Zhou, Y. Yang, L. Yuan, K. Yamato and B. Gong, *Org. Lett.*, 2011, **13**, 3798.
19 X. Li, Y. Fang, P. Deng, J. Hu, T. Li, W. Feng and L. Yuan, *Org. Lett.*, 2011, **13**, 4628.
20 J. H. Esch and B. L. Feringa, *Angew. Chem., Int. Ed.*, 2000, **39**, 2263.
21 A. R. Hirst, B. Escuder, J. F. Miravet and D. K. Smith, *Angew. Chem., Int. Ed.*, 2008, **47**, 8002.
22 H. L. Liu, P. C. Zhang, M. J. Liu, S. T. Wang and L. Jiang, *Adv. Mater.*, 2013, **25**, 4477.
23 P. D. Wadhavane, R. E. Galian, M. A. Izquierdo, J. Aguilera-Sigalat, F. Galindo, L. Schmidt, M. I. Burguete, J. Pérez-Prieto and S. V. Luis, *J. Am. Chem. Soc.*, 2012, **134**, 20554.
24 C.-T. Chen, C.-H. Chen and T.-G. Ong, *J. Am. Chem. Soc.*, 2013, **135**, 5294.
25 C. Caltagirone and P. A. Gale, *Chem. Soc. Rev.*, 2009, **38**, 520.
26 S. Kubik, *Chem. Soc. Rev.*, 2009, **38**, 585.
27 P. A. Gale, R. Pérez-Tomás and R. Quesada, *Acc. Chem. Res.*, 2013, **46**, 2801.
28 S. V. Krivovichev, O. Mentré, O. I. Siidra, M. Colmont and S. K. Filatov, *Chem. Rev.*, 2013, **113**, 6459.
29 P. A. Gale, *Acc. Chem. Res.*, 2011, **44**, 216.
30 Y. M. Yang, Q. Zhao, W. Feng and F. Y. Li, *Chem. Rev.*, 2013, **113**, 192.
31 B. Wu, F. Cui, Y. Lei, S. Li, N. de Sousa Amadeu, C. Janiak, Y.-J. Lin, L.-H. Weng, Y.-Y. Wang and X.-J. Yang, *Angew. Chem., Int. Ed.*, 2013, **52**, 5096.
32 C. Jia, B. Wu, S. Li, X. Huang, Q. Zhao, Q.-S. Li and X.-J. Yang, *Angew. Chem., Int. Ed.*, 2011, **50**, 486.
33 B. Wu, C. Jia, X. Wang, S. Li, X. Huang and X.-J. Yang, *Org. Lett.*, 2012, **14**, 684.
34 C.-X. Lin, X.-F. Kong, Q.-S. Li, Z.-Z. Zhang, Y.-F. Yuan and F.-B. Xu, *CrystEngComm*, 2013, **15**, 6948.
35 H. Ou Yang, Y. Gao and Y. Yuan, *Tetrahedron Lett.*, 2013, **54**, 2964.
36 S. Jagtap, M. K. Yenkie, N. Labhsetwar and S. Rayalu, *Chem. Rev.*, 2012, **112**, 2454.
37 C. R. Wade, A. E. J. Broomsgrove, S. Aldridge and F. P. Gabbaï, *Chem. Rev.*, 2010, **110**, 3958.
38 M. Cametti and K. Rissanen, *Chem. Soc. Rev.*, 2013, **42**, 2016.
39 P. Rajamalli and E. Prasad, *Langmuir*, 2013, **29**, 1609.
40 P. Rajamalli and E. Prasad, *Org. Lett.*, 2011, **13**, 3714.
41 H. Maeda, Y. Haketa and T. Nakanishi, *J. Am. Chem. Soc.*, 2007, **129**, 13661.
42 J. E. A. Webb, M. J. Crossley, P. Turner and P. Thordarson, *J. Am. Chem. Soc.*, 2007, **129**, 7155.

43 Y. M. Zhang, Q. Lin, T. B. Wei, X. P. Qin and Y. Li, *Chem. Commun.*, 2009, 6074.
44 J. W. Liu, Y. Yang, C. F. Chen and J. T. Ma, *Langmuir*, 2010, **26**, 9040.
45 B. B. Shi, P. Zhang, T. B. Wei, H. Yao, Q. Lin and Y. M. Zhang, *Chem. Commun.*, 2013, **49**, 7812.
46 Q. Lin, Y. P. Fu, P. Chen, T. B. Wei and Y. M. Zhang, *Tetrahedron Lett.*, 2013, **54**, 5031.
47 Q. Lin, X. Liu, T. B. Wei and Y. M. Zhang, *Chem.–Asian J.*, 2013, **8**, 3015.
48 Q. Lin, X. Liu, T. B. Wei and Y. M. Zhang, *Sens. Actuators, B*, 2014, **190**, 459.
49 Y. M. Zhang, Q. Lin, T. B. Wei and D. D. Wang, *Sens. Actuators, B*, 2009, **137**, 447.
50 S. Y. Zhang and Y. Zhao, *ACS Nano*, 2011, **5**, 2637.
51 T. Kitahara, M. Shirakawa, S. I. Kawano, U. Beginn, N. Fujita and S. Shinkai, *J. Am. Chem. Soc.*, 2005, **127**, 14980.
52 M. Zhu, M. J. Yuan, X. F. Liu, J. L. Xu, J. Lv, C. S. Huang, H. B. Liu, Y. L. Li, S. Wang and D. B. Zhu, *Org. Lett.*, 2008, **10**, 1481.